


FULL PAPER

Open Access



Automatic selection of Dst storms and their seasonal variations in two versions of Dst in 50 years

N. Balan^{1,2*} , S. Tulasiram³, Y. Kamide^{2,4}, I. S. Batista¹, J. R. Souza¹, K. Shiokawa², P. K. Rajesh⁵ and N. J. Victor⁶

Abstract

A computer program is developed to automatically identify the geomagnetic storms in Dst index by applying four selection criteria that minimize non-storm-like fluctuations. The program is used to identify the storms in Kyoto Dst and USGS Dst in 50 years (1958–2007). The identified storms ($Dst_{Min} \leq -50$ nT) are used to investigate their seasonal variations. It is found that the overall seasonal variations of the storm parameters such as occurrence, average intensity (average Dst_{Min}) and average strength (average $\langle Dst_{MP} \rangle$) in both versions of Dst exhibit clear semiannual variations with equinoctial maxima and solstice minima; and the maxima and minima in intensity and strength ($\sim \pm 17\%$ each) are less than those in occurrence ($\sim \pm 28\%$). Wavelet spectra of the storms reveal the existence of distinct semiannual component in four solar cycles (SCs 20–23) and weak longer and shorter-period components in some SCs. The semiannual variation observed also in the mean energy input during the main phase (MP) of the storms estimated from Dst is interpreted in terms of the (1) equinoctial mechanism based on the varying angle between the Earth–Sun line and Earth’s dipole axis and (2) Russell–McPherron effect based on the varying angle between the GSM Z-axis and GSE Y-axis; and the yearly range of the dipole tilt angle μ (23.2°) involved in the equinoctial mechanism is found larger than the tilt angle θ (16.3°) involved in the RM effect.

Keywords: Geomagnetic Dst storms, Semiannual variation, Energy input, Ring current, Equinoctial hypothesis, RM effect

Background

Geomagnetic storms are disturbances in Earth’s magnetic field lasting from several hours to several days, and are produced by enhanced solar wind–magnetosphere coupling (e.g., Svalgaard 1977; Akasofu 1981; Gonzalez et al. 1994; Kamide et al. 1998) and ionosphere–magnetosphere plasma coupling (e.g., Daglis 1997; Khazanov et al. 2003; Ebihara et al. 2005). Geomagnetic indices such as the low-latitude Dst (disturbance storm time) index have been developed to study geomagnetic storms (e.g., Sugiura 1964; Sugiura and Kamei 1991; Love and Gannon 2009); see also Rostoker (1972). The storms have been studied for over 150 years using geomagnetic data, indices and models (e.g., Sabine 1856; Mayaud 1978; Iyemori

1980; Takalo et al. 1995; Siscoe and Crooker 1996; Daglis 1997; Kamide et al. 1998; Gonzalez et al. 1999; Cliver et al. 2000; Fok et al. 2001; Liemohn et al. 2001; O’Brien and McPherron 2002; Vijaya Lekshmi et al. 2011; Yakhovchouk et al. 2012; Zhao and Zong 2012; Katus and Liemohn 2013; Kumar et al. 2015; Lakhina and Tsuritani 2016). From these studies, it is known that the occurrence and intensity of the storms vary with solar activity, time of year and time of day.

The storms are frequent and intense at high levels of solar activity (e.g., Ellis 1899; Zhang et al. 2007) due to the frequent occurrence of CMEs and ICMEs (interplanetary CMEs) (e.g., Gopalswamy et al. 2005). During solar minimum, the interaction of co-rotating interaction regions (CIRs) of solar origin with the magnetosphere produces weak recurrent storms (e.g., Richardson et al. 2001; Tulasiram et al. 2010; Cramer et al. 2013). Geomagnetic storms undergo a semiannual

*Correspondence: balannan@gmail.com

² ISEE, Nagoya University, Furo-cho, Chikusa-ku, Nagoya 464-8601, Japan
Full list of author information is available at the end of the article

variation with equinoctial maxima and solstice minima (e.g., Cortie 1912; Cliver et al. 2000, 2001, 2004; Svalgaard et al. 2002; Svalgaard 2011). The semiannual variation has been interpreted in terms of the (1) axial hypothesis based on the variation of the heliospheric latitude of the Earth with time of year (e.g., Cortie 1912), (2) equinoctial hypothesis based on the variation of the angle between the Earth–Sun line and Earth’s dipole axis (e.g., Bartels 1932) and (3) Russell–McPherson (RM) effect based on the varying angle between the GSM (geocentric solar magnetospheric) Z -axis and GSE (geocentric solar ecliptic) Y -axis (Russell and McPherson 1973). Newell et al. (2001) suggested that both auroral ovals going simultaneously to darkness can cause the activity maximizing at equinoxes. Recently, Azpilicueta and Brunini (2012) suggested another version of the equinoctial hypothesis, that is, the deformation during the year of the shape of the magnetospheric cavity within which the ring current flows can cause the activity maximizing at equinoxes.

Recently, Mursula et al. (2011) found the global geomagnetic activity index (A_p) in 15 years in 1993–2008 showing a dominant annual variation, with equinoctial maxima alternating between spring in solar cycle (SC) 22 and fall in SC 23. Consequently they suggested that the overall semiannual variation in geomagnetic activity is due to the solar hemispheric asymmetry in the distribution of solar wind, which varies from one SC to another; and the overall semiannual variation has been seriously over estimated and is largely an artifact of the dominant annual variation with maxima alternating between spring and fall. However, using the inter-hourly variation (IHV) data for over 200 years Svalgaard (2011) contradicted this suggestion and showed that the semiannual variation is not an artifact. Thus, it is worth re-examining the semiannual variation in other indices.

In this paper, we present the seasonal variations of Dst storms in 50 years of Dst data. In addition to the widely used Kyoto Dst, the new (and improved) USGS Dst is used to check and confirm the findings. A brief comparison of the two Dst versions is presented in “**Dst data**” section. The storms in both versions are identified by developing a computer program (“**Storm identification**” section). The storms are analyzed for their important characteristics including the mean value of Dst during main phase (MP) (called $\langle \text{Dst}_{\text{MP}} \rangle$). Wavelet spectra of the storms are used to identify their periodic variations. The results are presented and discussed in “**Results**” and “**Discussion**” sections. Similar semiannual variations observed in both Dst versions are interpreted in terms of the equinoctial hypothesis and RM effect.

Dst data

We use the Kyoto Dst of 1 nT resolution available at <http://wdc.kugi.kyoto-u.ac.jp/dstdir/> and USGS Dst of 0.1 nT resolution available at <http://geomag.usgs.gov/data> for 50 years from 1958 to 2007. Both versions of the low-latitude hourly index (Dst) are obtained from the horizontal H component measured at four low-latitude stations (3 in north and 1 in south) outside the equatorial electrojet belt. The method of calculating Kyoto Dst (Sugiura 1964; Sugiura and Kamei 1991) involves (1) defining the baseline magnetic perturbation by a power series in time, (2) determining the solar quiet (Sq) variation for each observatory by selecting five quietest days for each month and using a double Fourier series as a function of local time and month, (3) obtaining the disturbance time variation [$D(t)$] for each observatory by removing the signals in (1) and (2) from the observed H component and (4) calculating Dst as the average of the four $D(t)$ values normalized to the dipole equator. Karinen and Mursula (2005; and references therein) reconstructed the Kyoto Dst for 1932–2002 using the H component data from Cape Town for 1932–1940, which is not available for the closest Dst station (Hermanus). They also pointed out some obvious errors in Kyoto Dst.

Following the same calculation algorithm of Sugiura (1964), Love and Gannon (2009) produced the USGS Dst, first introduced as $\text{Dst}^{5807-4\text{SH}}$. The two versions of Dst differ primarily in the removal of secular and Sq variations. While Kyoto Dst partially removes these variations, USGS Dst more fully removes them by using both time- and frequency-domain band-stop filtering that selectively removes the specific Fourier terms approximating periodic variations driven by Earth’s rotation, Moon’s orbit, Earth’s orbit around the Sun, and their mutual coupling. The resulting four disturbance time series are weighted by the observatory geomagnetic latitude and then averaged to get the USGS Dst. Love et al. (2015) used the Dst data for forecasting extreme geomagnetic storms. The Kyoto Dst data do not seem to be corrected for the excessive, seasonally varying quiet-time level, or the “non-storm component” which is unrelated to magnetic storms (Cliver et al. 2001; Karinen and Mursula 2006).

A comparison of the two Dst indices shows significant offset (or difference) between them, which is found to depend on short and long time scales (time of day, year and solar cycles) and level of Dst. The offset of Kyoto Dst compared to USGS Dst on the whole is -8.50 nT in all data together and -5.00 nT in quiet-time data ($\text{Dst} > -25$ nT) alone. The offset is mainly due to the different methods of removal of the secular and Sq variations (Sugiura and Kamei 1991; Love and Gannon 2009); detailed studies of the offset are beyond the scope of the present paper.

Storm identification

The storms are automatically identified by developing a computer program which minimizes non-storm-like fluctuations. Figure 1, for example, illustrates the procedure using Kyoto Dst. The program first detects the negative slopes in the Dst variation (green dots, Fig. 1a) and identifies the preliminary main phase onsets (MPOs) when Dst starts decreasing (red stars) and DstMin when Dst reaches maximum negative values during main phase (MP) of the storms (black stars) as shown in Fig. 1a. The program then applies the selection criterion (1): $Dst_{Min} \leq -50$ nT and MP duration > 2 h, and criterion (2): absolute value of MP range, that is, $|Dst_{MPO} - Dst_{Min}| \geq 50$ nT. By applying criteria (1) and (2), many short-period, non-storm-like negative fluctuations of Dst are eliminated (Fig. 1b). With a view to further avoid the short-period positive excursions in Dst during MP and to clearly identify the storms caused by separate drivers (ICMEs), the criterion (3), that is, separation between DstMin and next MPO ≥ 10 h is applied. This means that two storms separated by less than 10 h are treated as a single storm assuming that they are due to the same ICME, for example the change from Fig. 1b, c. Further to avoid very slowly varying, non-storm-like long duration decreases in Dst, the criterion (4), that is, rate of change in Dst during MP or $(dDst/dt)_{MP} < -5$ nT/h, is applied. By applying criteria (1)–(4), the computer program detects the two clear storms in Fig. 1c. The corresponding USGS Dst shown by red curve

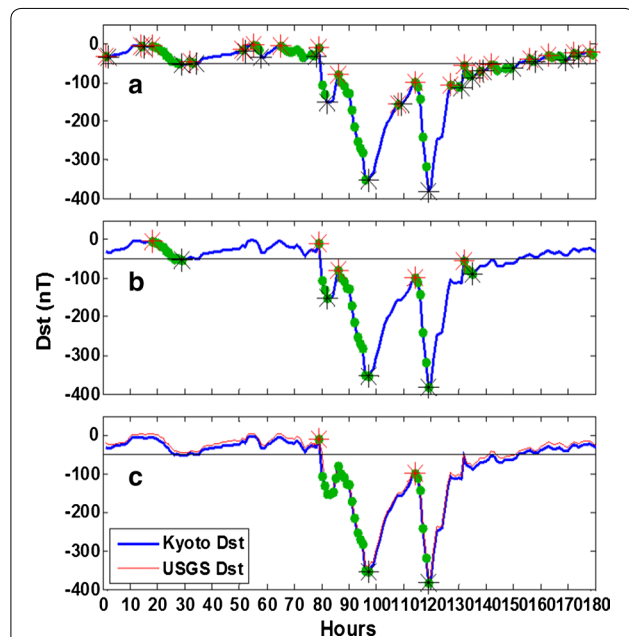


Fig. 1 An example of Kyoto Dst data (26 October–01 November 2003) illustrating the identification of Dst storms (a, b and c); USGS Dst data are also shown in c in red, see text

also shows the two storms, with no significant difference in this case.

Similar procedure is applied to both Kyoto Dst and USGS Dst data for the period 1958–2007. The program thus identified 761/585 storms in Kyoto Dst/USGS Dst, which include 34/33 super storms ($Dst_{Min} \leq -250$ nT), 296/210 intense storms ($-250 < Dst_{Min} \leq -100$ nT) and 431/342 moderate storms ($-100 < Dst_{Min} \leq -50$ nT). The storms on the whole are 30% more in Kyoto Dst than in USGS Dst mainly due to the base line offset between the two indices (“Dst data” section) as illustrated in Fig. 2 which shows examples of moderate (panel a) and intense (panel b) storms identified in Kyoto Dst but not in USGS Dst because for these storms DstMin in USGS Dst is greater than -50 and -100 nT. A test is made to see whether a constant shift of one of the indices by an amount equal to their average offset can give equal number of storms. As shown in Fig. 3a, the distribution of DstMin is similar in both indices, and shifting USGS Dst by the average overall offset of -8.5 nT increases the number of storms in it from 585 to 660 (Fig. 3b), which is still 99 storms less than those in Kyoto Dst. A constant shift does not give equal number of storms (Fig. 3b)

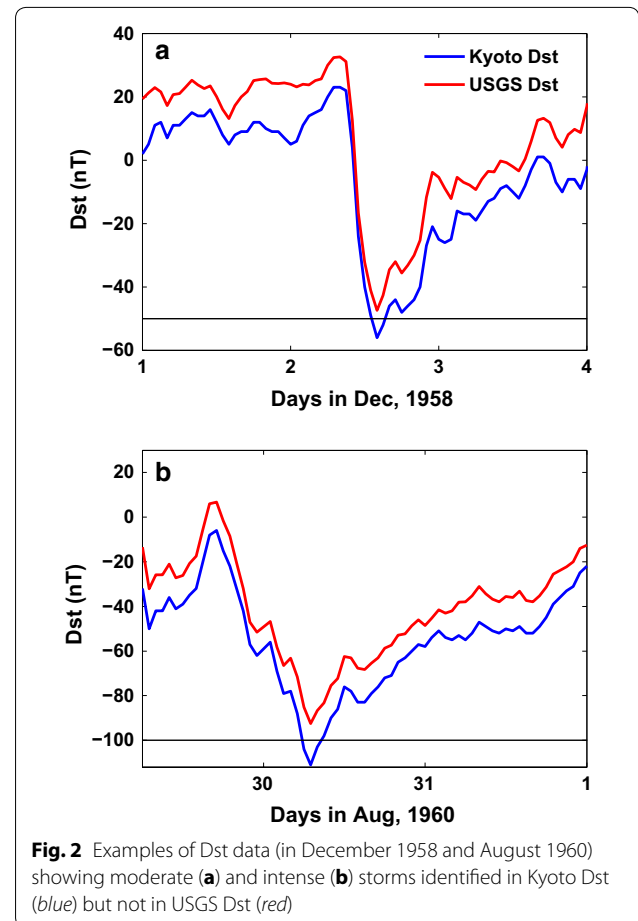
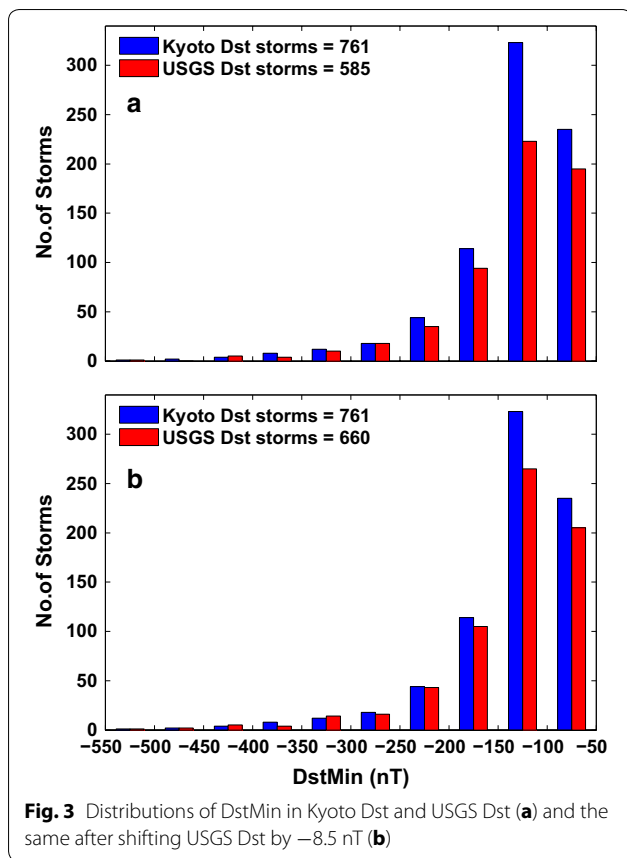


Fig. 2 Examples of dst data (in December 1958 and August 1960) showing moderate (a) and intense (b) storms identified in Kyoto Dst (blue) but not in USGS Dst (red)



because the offset varies with short and long time scales and level of Dst. As discussed, the number of storms in the two indices differs mainly due to their varying baseline offset.

Storm analysis

The identified storms are analyzed for their important characteristics. Main phase duration T_{MP} is the time interval between main phase onset (MPO) when Dst starts decreasing and DstMin. $\int_{T_{MP}} |Dst|dt$ is the integral (or sum) of the modulus of Dst from MPO to DstMin. Since energy input takes place during MP, the mean value of Dst during MP is calculated as $\langle Dst_{MP} \rangle = (-1/T_{MP}) \int_{T_{MP}} |Dst|dt$. It represents the impulsive strength (or strength in short) of Dst storms while DstMin represents their intensity (Balan et al. 2014). It ($\langle Dst_{MP} \rangle$) has been shown to be a unique parameter that can indicate the severity of space weather while the conventional parameter DstMin is insufficient (Balan et al. 2016). Average DstMin ($=\Sigma DstMin/\text{number of storms}$) and average $\langle Dst_{MP} \rangle = (\Sigma \langle Dst_{MP} \rangle / \text{number of storms})$ represent the average intensity and average strength of a certain number of storms during a specific period. Energy input in the ring current is estimated as

$E = ((dDst/dt)_{MP} + \alpha Dst_{MP})$ where $\alpha = 0.13$ is the ring current decay constant and Dst_{MP} in the second term is the mean of the two Dst values used for the first term (Burton et al. 1975; Stern 1984). Mean energy input during MP ($\langle E_{MP} \rangle = \int E_{MP} / T_{MP}$) is computed.

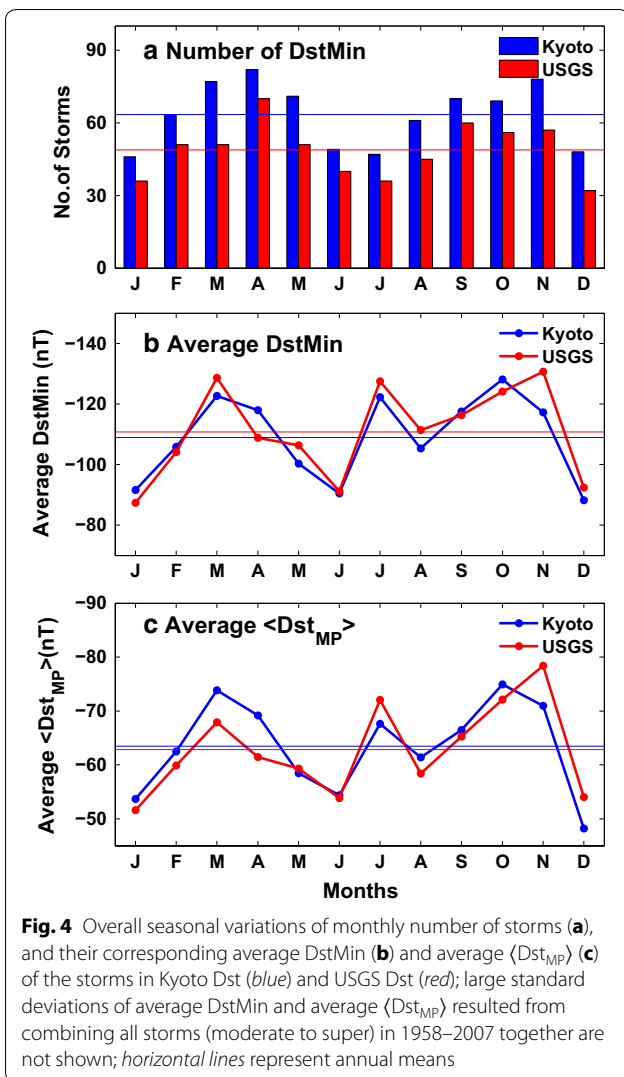
Results

The seasonal variations of the storm characteristics studied separately for super storms, intense storms and all storms together are found similar. So we consider all storms together in the rest of the paper for statistics.

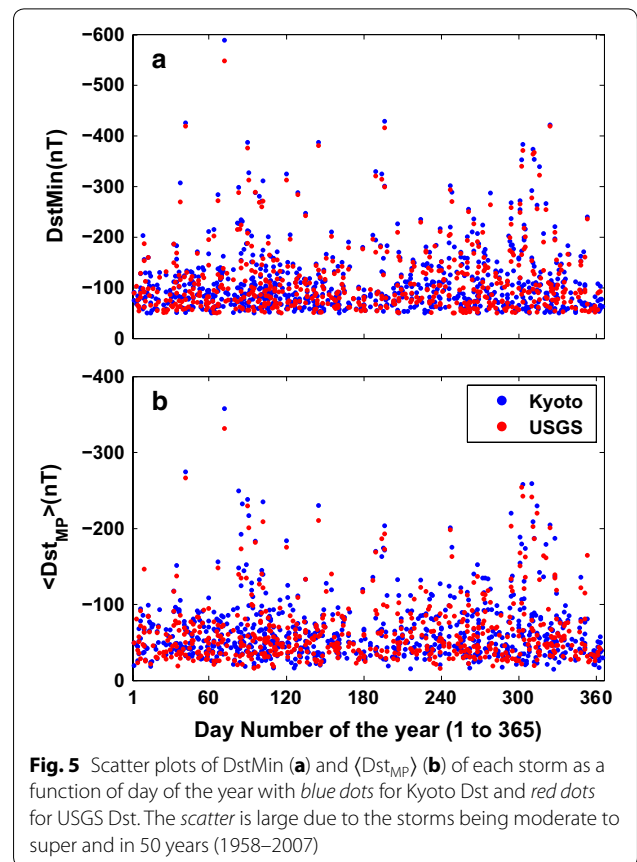
Seasonal variation

The overall seasonal variation of storm parameters is obtained by combining the storms in each month in 1958–2007, which gives a 12-point data series from January to December. Figure 4 shows the resulting seasonal variations of the monthly number of storms and their average DstMin and average $\langle Dst_{MP} \rangle$ in both versions of Dst; horizontal lines represent annual means; the large standard deviations resulted from combining all storms (moderate to super) together in 50 years are not plotted for better visibility. The main feature in Fig. 4 is the semiannual variation. All parameters in both versions of Dst exhibit similar semiannual variations with equinoctial maxima and solstice minima, though the September equinox maximum in occurrence in Kyoto Dst and intensity and strength in USGS Dst shift to the end of the equinox (early November) which seems possible since September equinox extends to 06 November as seasons are 91 (and 92) days long centered at the equinoxes and solstices days. Love and Gannon (2009) also found the intense storms ($DstMin < -100$ nT) generally occurring most likely in late equinoxes. There is also an unexpected secondary peak in the intensity and strength in July. It is found to be due the occurrence of 10 intense storms and 3 super storms ($DstMin$ up to -327 nT) in July while moderate storms generally occur in other June solstice months. Though such storms in July have been studied, for example in terms of strong ICMEs and fast solar wind and interplanetary magnetic clouds (e.g., Lepping et al. 2001), the reason(s) for their preference in July compared to other June solstice months seems not understood. Figure 5 shows scatter plots of DstMin and $\langle Dst_{MP} \rangle$ of each storm as a function of day of the year. The scatter is large due to the storms being moderate to super and in 50 years (1958–2007).

Using the data in Fig. 4, Table 1 lists the annual means, maxima at equinoxes and minima in solstices, and their percentage deviations from annual means. Seasonal averages, however, are not considered for the fluctuations in intensity and strength in July. As listed, the maxima and minima in occurrence (in percentage) are greater than those in intensity and strength, and the maxima (and



minima) are nearly equal except in USGS Dst in which the occurrence in June solstice (−18%) and strength at March equinox (8%) are comparatively small. Considering the averages of the two maxima and two minima, in Kyoto Dst, the number of storms is about 27% more at equinoctial maximum and 25% less in solstice minimum, and corresponding average DstMin is 16% greater and 18% smaller and average $\langle Dst_{MP} \rangle$ is 17% greater and 19% smaller. In USGS Dst, the number of storms is 32% more at equinoctial maximum and 27% less in solstice minimum, and corresponding average DstMin is 17% greater and 20% smaller and average $\langle Dst_{MP} \rangle$ is 17% greater and 16% smaller. These averages of corresponding parameters are nearly equal in the two indices. Considering the two indices together, the maxima and minima on the whole are $\sim \pm 28\%$ in occurrence and $\sim \pm 17\%$ in intensity and strength.



To investigate further, the seasonal variations of the number of storms are obtained separately for the 11-year solar cycles (SCs) 19–23 (Fig. 6). It shows clear semiannual variations in all four SCs (20–23) except in the partial data (1958–1964) in SC 19, though September equinox maxima in SCs 20–21 seem weaker than March equinox maxima and variations of period other than 6-months are also present. To investigate the periodic variations, the storms in the five SCs (Fig. 6) are joined to obtain a 60-point data series (5×12 , January 1958 to December 2007) of 1 month resolution, and its wavelet spectra are obtained (Fig. 7) using Morlet mother wavelet technique (Torrence and Compo 1998). The white lines in Fig. 7 indicate cone of confidence and black and purple curves represent 95 and 98% significance levels. As shown by the spectra, clear and distinct semiannual component is present in all 4 SCs (20–23) with amplitude up to 12 storms in Kyoto Dst and 10 storms in USGS Dst. A weak component close to annual period (9–12 months) is also present in two SCs (20–21) with amplitude up to 8 storms in Kyoto Dst and 6 storms in USGS Dst. A long-period (~ 15 months) component centered in SC 21 and a short-period (~ 3 months) component in some SCs are also present.

Table 1 Semiannual maxima and minima of storm parameters

Storm type	Number of storms		Average DstMin (nT)		Average $\langle \text{Dst}_{\text{MP}} \rangle$ (nT)	
	Kyoto (%)	USGS (%)	Kyoto (%)	USGS (%)	Kyoto (%)	USGS (%)
Annual mean	63	49	-108.9	-110.7	-63.5	-62.8
March	82 (+30)	70 (+42)	-122.7 (+13)	-128.6 (+16)	-73.9 (+16)	-67.9 (+8)
October	78 (+24)	60 (+22)	-128.1 (+18)	-130.7 (+18)	-74.9 (+18)	-78.4 (+25)
June	49 (-22)	40 (-18)	-90.5 (-17)	-91.1 (-18)	-54.4 (-14)	-53.8 (-14)
December	46 (-27)	32 (-35)	-88.2 (-19)	-87.4 (-21)	-48.2 (-24)	-51.6 (-18)

List of annual means, and equinoctial maxima and solstice minima of the number of storms, average DstMin and average $\langle \text{Dst}_{\text{MP}} \rangle$ and their percentage deviations (in brackets) from the annual means in Kyoto Dst and USGS Dst by considering all storms in 1958–2007

Discussion

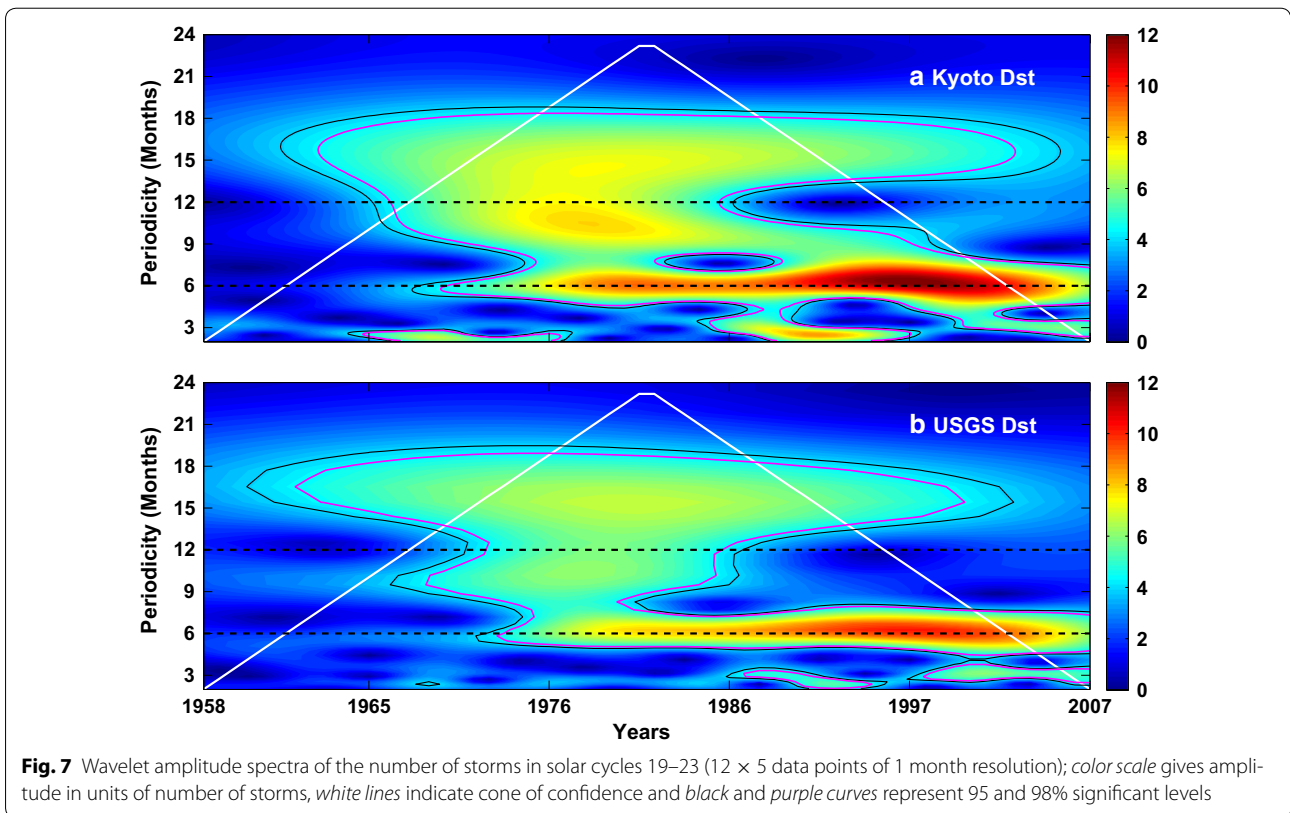
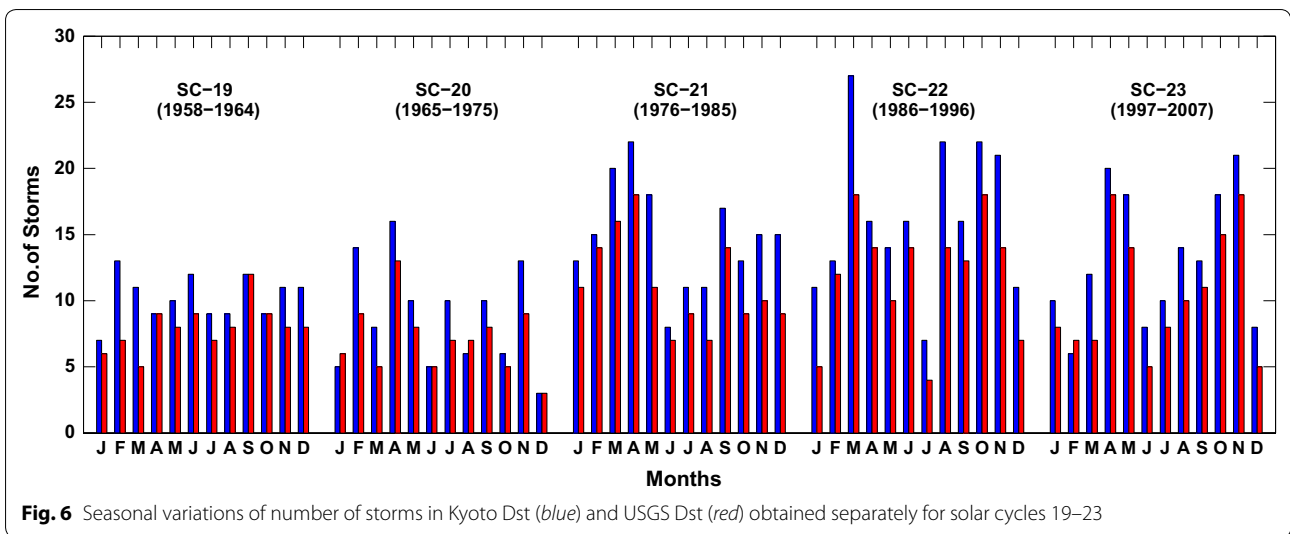
The important results are discussed. A computer program is developed to identify the geomagnetic storms in Dst data (“Storm identification” section). Using four selection criteria, the program identified about 24 and 35% of the storms in 50 years (1958–2007) in Kyoto Dst and USGS Dst, respectively, compared to those (3187 and 1870) that would have been identified if the usual procedure based on criterion 1 ($\text{DstMin} \leq -50$ nT and MP duration >2 h) alone were used. The new selection procedure largely minimized the non-storm-like fluctuations in both versions of Dst. These are major advantages of the automated storm selection procedure. Recently, Katus and Liemohn (2013) reported another automated storm selection procedure. It involves searching for negative peaks in Dst ($\text{DstMin} < -50$ nT), finding the maximum Dst within 24 h prior to DstMin for MPO and 96 h after DstMin for the end of recovery phase, and looking for a sharp increase in Dst within 8 h prior to MPO for storm sudden commencement (SSC). Using this procedure Katus and Liemohn (2013) identified 697 storms in Kyoto Dst in 24 years (1985–2009) while the present procedure identified nearly the same number of storms (761) but in 50 years (1958–2007).

The identified storms are 30% more in Kyoto Dst (761) than in USGS Dst (587) mainly due to the baseline offset (or difference) between the two indices that arises from the different methods of removal of the secular and Sq variations calculated in different ways in the two indices (e.g., Sugiura and Kamei 1991; Love and Gannon 2009), which also leads to storm time differences (Fig. 2). A constant shift of one of the Dst versions by their average offset (8.5 nT) cannot give equal number of storms (Fig. 3) because the offset varies with short and long times scales and level of Dst. Detailed studies of the offset are beyond the scope of the present paper. Katus and Liemohn (2013) also found large differences between the storms in Kyoto Dst, USGS Dst and SYM-H indices especially at DstMin, on average up to 20% of the peak DstMin, though the storms in the indices are highly correlated.

Irrespective of the offset, the overall seasonal variation of occurrence of the storms in both versions of Dst in 50 years exhibits nearly equal ($\sim \pm 28\%$) semiannual patterns (Fig. 4) with maxima at equinoxes and minima in solstices. Unlike in earlier studies, the average intensity and average strength of the storms (average DstMin and average $\langle \text{Dst}_{\text{MP}} \rangle$) used in the present study also exhibit clear semiannual variations though with reduced maxima and minima ($\sim \pm 17\%$). The monthly occurrence of the storms in the five 11-year SCs 19–23 considered separately also show clear semiannual variation in all four SCs 20–24 (Fig. 6). Wavelet spectra of these data reveal the presence of weak longer- and shorter-period components in some SCs in addition to the clear and distinct semiannual component (Fig. 7). However, the long-period components (around annual period, 9–15 months) are not found to alternate between spring and fall in successive SCs as was observed in Ap index in 1993–2008 (Mursula et al. 2011), maybe because the ring current index Dst and global geomagnetic activity index Ap have somewhat different properties and drivers.

Mechanisms

Of the different possibilities introduced in “Background” section, the equinoctial hypothesis (Bartels 1932) and RM effect (Russell and McPherron 1973) are usually used to explain the semiannual variation. Both mechanisms involve solar wind–magnetosphere coupling through the connection (and reconnection) mechanism between IMF Bz and magnetopause magnetic field (e.g., Dungey 1961), though the mechanism was not known at the time of proposal of the equinoctial hypothesis. Cliver et al. (2000) argued that while the RM effect causes stronger maxima at equinoxes (such as mountain building) the equinoctial hypothesis can cause deeper minima in solstices (such as valley digging). O’Brien and McPherron (2002) showed that the RM effect is present though the enhancements in the Dst index exhibit a seasonal pattern that is significantly different from the RM effect.



We attempt to connect the observed semiannual variation with equinoctial hypothesis and RM effect. Equinoctial hypothesis involves the variation of Earth’s dipole tilt angle μ with respect to the GSM Z-axis in X–Z plane where X points toward Sun from Earth. The tilt angle (μ) varies (i) between $\pm 23.5^\circ$ with time of year due to the tilt of Earth’s axis of rotation with respect to solar ecliptic plane and (ii) between $\pm 11.2^\circ$ with time of day due to the

tilt of Earth’s dipole axis from its rotation axis. The total tilt μ of the dipole axis is therefore the sum of (i) and (ii), which varies between $\pm 34.7^\circ$ within a year with positive sign toward the Sun (in northern hemisphere) and negative sign away from the Sun. The RM effect involves the varying angle θ of the Earth’s dipole axis with respect to GSE (geocentric solar ecliptic) Y-axis in the plane perpendicular to the Earth–Sun line. The angle θ varies

between 53° and 90° within a year. The variations of μ and θ with time of the day (UT hours) and year (days) were presented by O'Brien and McPherron (2002).

The reconnection mechanism that controls the intensity and strength of geomagnetic storms becomes most effective when the tilt angles μ and θ are minimum (e.g., Crooker and Siscoe 1986; Borovsky et al. 2008; Cnossen et al. 2012). Russell et al. (2003) showed that for Bz due southward (or IMF clock angle of 180°), the neutral line length where IMF Bz is anti-parallel to Earth's dipole field and where magnetic reconnection occurs extends over a wide longitudinal width of ~170° at $\mu = 0$ and decreases with increasing absolute value of μ . As for θ , when it is a minimum, the average Parker spiral tends to present large component of southward IMF Bz anti-parallel to Earth's dipole causing large day-side reconnection and energy transfer into the magnetosphere. It is therefore expected to observe frequent occurrence of Dst storms and larger DstMin for smaller values of absolute tilt angles μ and θ due to enhanced magnetospheric energy input. The energy input in the ring current during MP estimated from Dst (Fig. 8) exhibits similar semiannual variation as the storm parameters (Figs. 4, 5, 6, 7), which further confirm the dipole tilt angle control on ring current and geomagnetic activity.

As shown in Fig. 9, the seasonal variations of daily mean tilt angles μ and θ and number of storms exhibit nearly same semiannual patterns. The maxima/minima in the number of storms seem to correspond to the minima/maxima in the tilt angles though there is a slight shift by 1 month. Similar shift has been reported in ionospheric equinoctial maxima and solstice minima (e.g., Balan et al. 1998), which seems to have its effects on the seasonal variation of Dst storms through ionosphere–ring current coupling. The results in Figs. 4, 5, 6, 7, 8

and 9 therefore indicate that the semiannual variation of Dst storms is real and can be attributed to the variation of Earth's dipole tilt angles μ and θ and their control on the magnetic reconnection rate, as was established earlier using over 200 years of IHV data (Svalgaard 2011). However, μ exhibits larger (23.2°, from 0.2° to 23.4°) variation over a year than θ (16.3°, from 66.6° to 82.9°) (Fig. 9) which seems indicating probably the larger control of μ on semiannual variation than θ provided the reconnection rates per degree of μ and θ are equal which needs to be validated through model calculations.

The larger possible control of equinoctial hypothesis than RM effect was in fact suggested earlier by Cliver et al. (2000, 2001) and O'Brien and McPherron (2002). Cliver et al. (2000) showed that while RM effect accounts for the observed higher geomagnetic activity in March and September bulk of the semiannual variation (~65%) results from the equinoctial hypothesis that causes lower geomagnetic activity in solstices. In another paper using 40 years of Kyoto Dst (1957–1997), Cliver et al. (2001) estimated that the amplitude of the storm component of semiannual variation is only ~30–50% while the remaining ~50–70% results from non-storm component. They also showed that the equinoctial hypothesis appears to dominate the storm component by 20–40% while only ~10% accounts for the combined axial/RM effect. They also suggested candidate mechanisms for the non-storm component including the Malin–Isikara effect (the seasonal displacement of ring/tail currents by solar wind compression) (Malin and Isikara 1976) and a semiannual variation of magnetopause currents. O'Brien and McPherron (2002) showed that the enhancements in the Dst exhibit seasonal and diurnal patterns that are significantly different from the RM effect.

In addition to the CME–magnetosphere coupling, ionosphere–ring current coupling (e.g., Fok et al. 2001; Liemohn et al. 2001; Ebihara et al. 2005) can also contribute to the observed semiannual variation as the ionosphere exhibits strong semiannual variation under both magnetically quiet and active conditions (e.g., Balan et al. 1998, 2011). It is important to carry out modeling studies to evaluate the relative importance of the equinoctial hypothesis, RM effect and ionosphere–ring current coupling on the observed semiannual variation of Dst storms. However, such modeling studies are beyond the scope of the present paper.

Conclusions

Seasonal variation of geomagnetic storm parameters in Kyoto Dst and USGS Dst is studied using 50 years (1958–2007) of data. The storms are identified by a computer program that minimizes non-storm-like fluctuations by applying four selection criteria. The program identified

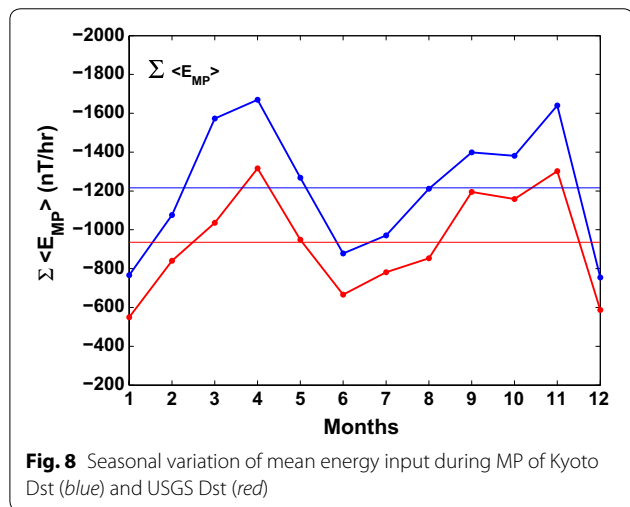
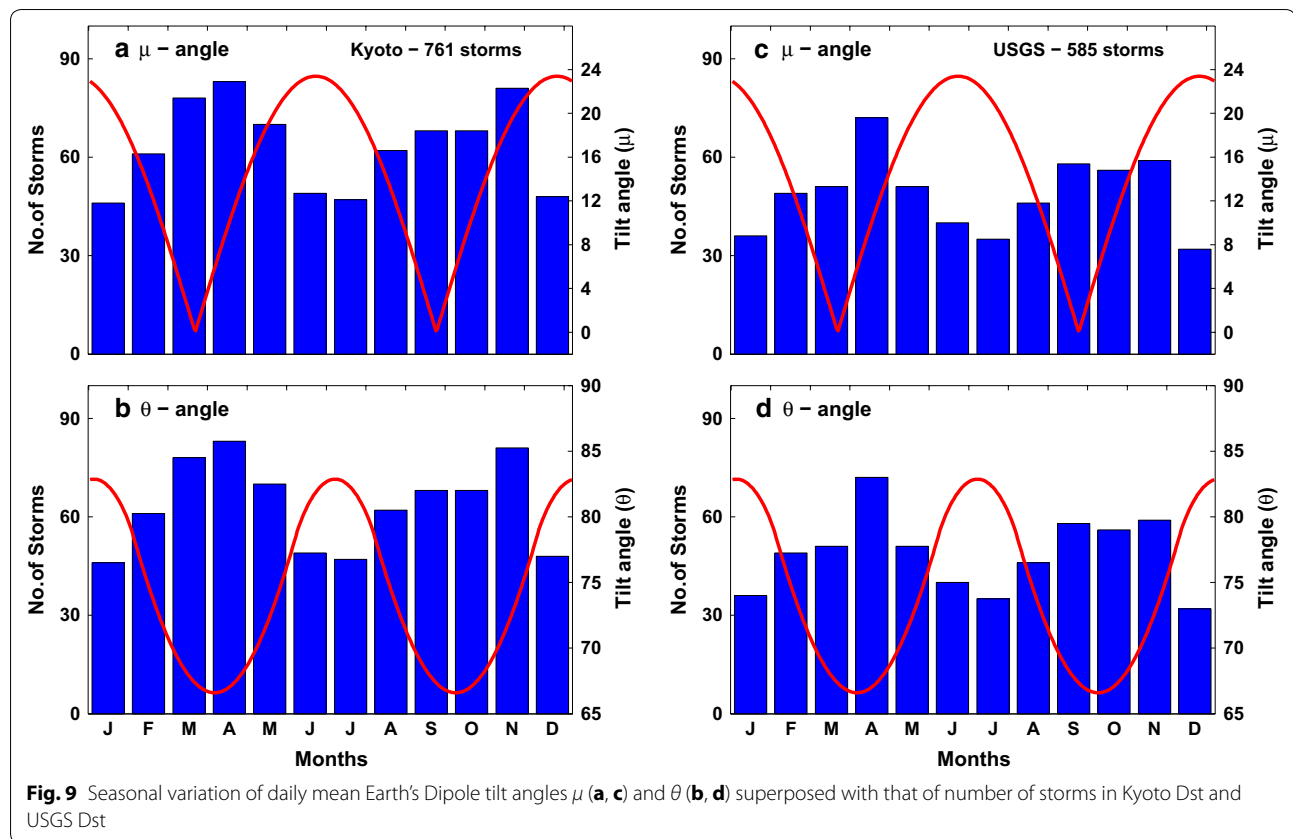


Fig. 8 Seasonal variation of mean energy input during MP of Kyoto Dst (blue) and USGS Dst (red)



761/585 storms in Kyoto Dst/USGS Dst, which include 34/33 super storms ($\text{DstMin} \leq -250$ nT), 296/210 intense storms ($-250 < \text{DstMin} \leq -100$ nT) and 431/342 moderate storms ($-100 < \text{DstMin} \leq -50$ nT). The storms are 30% more in Kyoto Dst mainly due to its varying baseline offset (or difference) compared to USGS Dst due to the different methods of removal of the secular and Sq variations in the two indices. The offset that varies with short and long time scales (time of day, year and solar cycles) and level of Dst on the average is -8.50 nT in all data and -5.00 nT in quiet-time ($\text{Dst} > -25$ nT) data.

The storms are analyzed for their important characteristics including the mean value of Dst during the main phase ($\langle \text{Dst}_{\text{MP}} \rangle$). Irrespective of the difference between the two Dst indices, the overall seasonal variation of the storms in both indices show clear semiannual variations not only in occurrence but also in average intensity (average DstMin) and average strength (average $\langle \text{Dst}_{\text{MP}} \rangle$) with equinoctial maxima and solstice minima though the maxima and minima in intensity and strength ($\sim \pm 17\%$ each) are less than those in occurrence ($\sim \pm 28\%$). Wavelet spectra of the storms reveal the existence of distinct semiannual component in four solar cycles (SCs 20–23) and weak longer- and shorter-period components in some SCs. The semiannual variations observed also in

the mean energy input during MP obtained from Dst are consistent with the variations of the daily mean Earth's dipole tilt angle μ involved in the equinoctial hypothesis and θ involved in the RM effect. Though both mechanisms can account for the observed semiannual variations, the yearly range of μ (23.2° , from 0.2° to 23.4°) is larger than that of θ (16.3° , from 66.6° to 82.9°). Both versions of Dst seem to confirm that the semiannual variation of Dst storms is real.

Authors' contributions

NB initiated the study and prepared the paper. ST developed the computer program, did most of the data analysis and participated in the preparation of the paper. PKR, NJV and JRS are also involved in data analysis. YK, ISB and KS are involved in the discussions and preparation of the paper. All authors read and approved the final manuscript.

Author details

¹ INPE, Sao Jose dos Campos, SP CEP 12227-010, Brazil. ² ISEE, Nagoya University, Furo-cho, Chikusa-ku, Nagoya 464-8601, Japan. ³ Indian Institute of Geomagnetism, Navi Mumbai, India. ⁴ Rikubetsu Space and Earth Science Museum, Rikubetsu 049-4301, Japan. ⁵ National Cheng Kung University, Tainan, Taiwan. ⁶ Equatorial Geophysical Research Laboratory, IIG, Tirunelveli, India.

Acknowledgements

We thank Kyoto WDC (<http://wdc.kugi.kyoto-u.ac.jp/dstdir/>) and USGS (<http://geomag.usgs.gov/data>) for the Dst data. N. Balan thanks CNPq of Brazil (Grants 400373/2014-9 and 303461/2014-4) and ISEE of Nagoya University Japan (Grants JSPS KEKENHI (JP 15H05815 and JP 1606286)) for invitation fellowships.

Competing interests

The authors declare that they have no competing interests.

Funding

N Balan thanks CNPq of Brazil (Grants 400373/2014-9 and 303461/2014-4) and ISEE of Nagoya University Japan (Grants JSPS KEKENDHI (JP 15H05815 and JP 1606286) for invitation fellowships.

Publisher's Note

Springer Nature remains neutral with regard to jurisdictional claims in published maps and institutional affiliations.

Received: 14 October 2016 Accepted: 12 April 2017

Published online: 26 April 2017

References

- Akasofu S-I (1981) The energy coupling between the solar wind and the magnetosphere. *Space Sci Rev* 28:121
- Azpilicueta F, Brunini C (2012) A different interpretation of the annual and semiannual anomalies on the magnetic activity over the Earth. *J Geophys Res* 117:A08202. doi:10.1029/2012JA017893
- Balan N, Otsuka Y, Bailey GJ, Fukao S (1998) Equinoctial asymmetries in the ionosphere and thermosphere observed by the MU radar. *J Geophys Res* 103:9481
- Balan N, Yamamoto M, Liu JY, Otsuka Y, Liu H, Luhr H (2011) New aspects of thermospheric and ionospheric storms revealed by CHAMP. *J Geophys Res* 116:A07305. doi:10.1029/2010JA0160399
- Balan N, Skoug R, Tulasiram S, Rajesh PK, Shiokawa K, Otsuka Y, Batista IS, Ebihara Y, Nakamura T (2014) CME front and severe space weather. *J Geophys Res*. doi:10.1002/2014JA020151
- Balan N, Batista IS, Tulasiram S, Rajesh PK (2016) A new geomagnetic storm parameter for the severity of space weather. *Geosci Lett* 3:1–5. doi:10.1186/s40562-016-0036
- Bartels J (1932) Terrestrial-magnetic activity and its relation to solar phenomena. *Terr Magn Atmos Electr* 37:1
- Borovsky JE, Hesse M, Birn J, Kuznetsova MM (2008) What determines the reconnection rate at the dayside magnetosphere? *J Geophys Res* 113:A07210. doi:10.1029/2007JA012645
- Burton RK, McPherron RL, Russell CT (1975) An empirical relationship between interplanetary conditions and Dst. *J Geophys Res* 80:4204–4214
- Cliver E, Kamide Y, Ling AG (2000) Mountains versus valleys: semiannual variation of geomagnetic activity. *J Geophys Res* 105(A2):2413. doi:10.1029/1999JA900439
- Cliver E, Kamide Y, Ling AG, Yokoyama N (2001) Semiannual variation of the geomagnetic Dst index: evidence for a dominant nonstorm component. *J Geophys Res* 106:21297–21304
- Cliver E, Svalgaard WL, Ling AG (2004) Origins of the semiannual variation of geomagnetic activity in 1954 and 1996. *Ann Geophys* 22(1):93–100. doi:10.5194/angeo-22-93
- Cnossen I, Wiltberger M, Ouellette JE (2012) The effects of seasonal and diurnal variations in the Earth's magnetic dipole orientation on solar wind–magnetosphere–ionosphere coupling. *J Geophys Res* 117:A11211. doi:10.1029/2012JA017825
- Cortie AL (1912) Sunspots and terrestrial magnetic phenomena, 1898–1911: the cause of the annual variation in magnetic disturbances. *Mon Not R Astron Soc* 73:52
- Cramer WD, Turner NE, Fok M-C, Buzulukova NY (2013) Effects of different geomagnetic storm drivers on the ring current: CRICM results. *J Geophys Res*. doi:10.1002/jgra.50138
- Crooker NU, Siscoe GL (1986) On the limits of energy transfer through dayside merging. *J Geophys Res* 91(A12):13393–13397
- Daglis IA (1997) The role of magnetosphere–ionosphere coupling in magnetic storm dynamics. In: Tsurutani BT et al (eds) *Magnetic storms*. Geophysical monograph series, vol 98. AGU, Washington, DC, pp 107–116
- Dungey JW (1961) Interplanetary magnetic field and the auroral zones. *Phys Rev Lett* 6:47–49
- Ebihara Y, Fok M-C, Sazykin S, Thomsen MF, Hairston RM, Evans DS, Rich FJ, Ejiri M (2005) Ring current and the magnetosphere–ionosphere coupling during the super storm of 20 November 2003. *J Geophys Res* 110:A09S22. doi:10.1029/2004JA010924
- Ellis W (1899) On the relation between magnetic disturbance and the period of solar spot frequency. *Mon Not R Astron Soc* 60:142–157
- Fok M-C, Wolf RA, Spiro RW, Moore TE (2001) Comprehensive computational model of Earth's ring current. *J Geophys Res* 106:8417
- Gonzalez WD, Joselyn JA, Kamide Y, Kroehl HW, Rostoker G, Tsurutani TB, Vasyliunas VM (1994) What is a geomagnetic storm? *J Geophys Res* 99:5771
- Gonzalez WD, Tsurutani TB, Clua de Gonzalez ALC (1999) Interplanetary origin of geomagnetic storms. *Space Sci Rev* 88:529
- Gopalswamy N, Yashiro S, Michalek G, Xie H, Lepping RP, Howard RA (2005) Solar source of the largest geomagnetic storm of cycle 23. *Geophys Res Lett* 32:L12S09. doi:10.1029/2004GL021639
- Iyemori T (1980) Time delay of the substorm onset from the IMF southward turning. *J Geomagn Geoelectr* 32:267
- Kamide Y et al (1998) Current understanding of magnetic storms: storm–substorm relationships. *J Geophys Res* 103(17):705. doi:10.1029/98JA01426
- Karinen A, Mursula K (2005) A new reconstruction of the Dst index for 1932–2002. *Ann Geophys* 23(475–485):2005
- Karinen A, Mursula K (2006) Correcting the Dst index: consequences for absolute level and correlations. *J Geophys Res* 111:A08207. doi:10.1029/2005JA011299
- Katus RM, Liemohn MW (2013) Similarities and differences in low-to middle-latitude geomagnetic indices. *J Geophys Res* 118:5149–5156. doi:10.1002/jgra.50501
- Khazanov GV, Liemohn MW, Newman TS, Fok M-C, Spiro RW (2003) Self-consistent magnetospheric–ionospheric coupling: theoretical studies. *J Geophys Res* 108(A3):1122. doi:10.1029/2002JA009624
- Kumar SB, Veenadhari B, Tulasiram S, Selvakumaran R, Mukherjee S, Singh R, Kadam BD (2015) Estimation of interplanetary electric field conditions for historical geomagnetic storms. *J Geophys Res*. doi:10.1002/2015JA021661
- Lakhina GS, Tsurutani BT (2016) Geomagnetic storms: historical perspective to modern view. *Geosci Lett* 3:5. doi:10.1186/s40562-016-0037-4
- Lepping RP et al (2001) The Bastille day magnetic clouds and upstream shocks: near-Earth interplanetary observations. *Sol Phys* 204:287–305
- Liemohn MW, Kozyra JU, Thomsen MF, Roeder JL, Lu G, Borovsky JE, Cayton TE (2001) Dominant role of the asymmetric ring current in producing the storm time Dst*. *J Geophys Res* 106(10):883
- Love JJ, Gannon JL (2009) Revised Dst and the epicycles of magnetic disturbance: 1958–2007. *Ann Geophys* 28(8):3101–3131. doi:10.5194/angeo-27-3101
- Love JJ, Rigler EJ, Pulkkinen A, Riley P (2015) On the lognormality of historical magnetic storm intensity statistics: implications for extreme-event probabilities. *Geophys Res Lett* 42:6544
- Malin SRC, Isikara AM (1976) Annual variation of the geomagnetic field. *Geophys J R Astron Soc* 17:445
- Mayaud PN (1978) The annual and daily variations of the Dst index. *Geophys J R Astron Soc* 55:193–201
- Mursula K, Tanskanen E, Love JJ (2011) Spring–fall asymmetry of substorm strength, geomagnetic activity and solar wind: implications for semiannual variation and solar hemispheric asymmetry. *Geophys Res Lett* 38:L06104. doi:10.1029/2011GL046751
- Newell PT, Meng C-I, Sotirelis T, Liou K (2001) Polar Ultraviolet Imager observations of global aurora power as a function of polar cap size and magnetotail stretching. *J Geophys Res* 106(A4):5895. doi:10.1029/2000JA003034
- O'Brien TP, McPherron RL (2002) Seasonal and diurnal variation of Dst dynamics. *J Geophys Res* 107(A11):1341. doi:10.1029/2002JA009435
- Richardson IG, Cliver EW, Cane HV (2001) Sources of geomagnetic storms for solar minimum and maximum conditions during 1972–2000. *Geophys Res Lett* 28:13. doi:10.1029/2001GL013052
- Rostoker G (1972) Geomagnetic indices. *Rev Geophys* 10:935
- Russell CT, McPherron RL (1973) Semiannual variation of geomagnetic activity. *J Geophys Res* 78:92
- Russell CT, Wang YL, Raeder J (2003) Possible dipole tilt dependence of day-side magnetopause reconnection. *Geophys Res Lett* 30:1937. doi:10.1029/2003GL017725

- Sabine E (1856) On the periodical laws discoverable in the mean effects of the large geomagnetic disturbances. *Philos Trans R Soc Lond* 146:357
- Siscoe G, Crooker N (1996) Diurnal oscillation of Dst: a manifestation of the Russell–McPherron effect. *J Geophys Res* 101:24985–24989
- Stern DP (1984) Energetics of the magnetosphere. *Space Sci Rev* 39:193–213
- Sugiura M (1964) Hourly values of equatorial Dst for the IGY. *Ann Int Geophys Year* 35:9–45
- Sugiura M, Kamei T (1991) Equatorial Dst index 1957–1957–1986. In: Berthelier A, Menvielle M (eds) IAGA bull 40. International Service of Geomagnetic Indices, Saint-Maur-des-Fosses
- Svalgaard L (1977) Geomagnetic activity: dependence on solar wind parameters. In: Zirker JB (ed) *Coronal holes and high speed wind streams*. Colorado Association University Press, Boulder, pp 371–441
- Svalgaard L (2011) Geomagnetic semiannual variation is not overestimated and is not an artifact of systematic solar hemispheric asymmetry. *Geophys Res Lett* 38:L16107. doi:10.1029/2011GL048616
- Svalgaard L, Cliver EW, Ling AG (2002) The semiannual variation of great geomagnetic storms. *Geophys Res Lett* 29(16):1765. doi:10.1029/2001GL014145
- Takalo J, Lohikoski R, Timonen J (1995) Structure function as a tool in AE and Dst time series analysis. *Geophys Res Lett* 22:635–638
- Torrence C, Compo GP (1998) A practical guide to wavelet analysis. *Bull Am Meteorol Soc* 79:61–78
- Tulasiram S, Liu CH, Su S-Y (2010) Periodic solar wind forcing due to recurrent coronal holes during 1996–2009 and its impact on Earth's geomagnetic and ionospheric properties during the extreme solar minimum. *J Geophys Res* 115:A12340. doi:10.1029/2010JA015800
- Vijaya Lekshmi D, Balan N, Tulasiram S, Liu JY (2011) Statistics of geomagnetic storms and ionospheric storms at low and mid latitudes in two solar cycles. *J Geophys Res* 116:A11328. doi:10.1029/2011JA017042
- Yakovchouk OS, Mursula K, Holappa L, Veselovsky IS, Karinen A (2012) Average properties of geomagnetic storms in 1932–2009. *J Geophys Res* 117:A03201. doi:10.1029/2011JA017093
- Zhang J et al (2007) Solar and interplanetary sources of major geomagnetic storms (Dst < −100 nT) during 1996–2005. *J Geophys Res* 112:A10102. doi:10.1029/2007JA012321
- Zhao H, Zong QG (2012) Seasonal and diurnal variation of geomagnetic activity: Russell–McPherron effect during different IMF polarity and/or extreme solar wind conditions. *J Geophys Res* 117:A11222. doi:10.1029/2012JA017845

Submit your manuscript to a SpringerOpen[®] journal and benefit from:

- Convenient online submission
- Rigorous peer review
- Immediate publication on acceptance
- Open access: articles freely available online
- High visibility within the field
- Retaining the copyright to your article

Submit your next manuscript at ► springeropen.com
